A Partial Digital Map of a Segment Within the Larval *Drosophila* Ventral Nerve Cord

David Allen Ariew
Charlottesville, VA

B.A. Philosophy, B.S. Neuroscience
The College of William and Mary
2008

A Thesis presented to the Graduate Faculty
of the University of Virginia in Candidacy for the Degree of
Master of Science

Department of Biology

University of Virginia
August, 2010

Abstract

Neuromics, the study of complete neuronal morphological maps of the brain, and connectomics, the study of complete neuronal connectivity maps, are rapidly evolving fields. Previous efforts have focused on simple systems, such as *C. elegans*, the only complete neuronal set ever characterized. While these efforts were monumental, our current interest is in global morphological characterization, or the neurome, rather than a map of the connectome (a neuronal wiring diagram); *C. elegans* has simplistic neurons that do not show great morphological variation, so this system is not our ideal. *Drosophila*, on the other hand, displays significant neuronal diversity, and also represents one of the greatest physiological, morphological, and genetic bodies of knowledge. *Drosophila* larvae, in particular, strike a good balance between variation and simplicity, as their nerve cords are bilaterally symmetric repeated segments, but with diverse and intricate neurons. Using the Condron lab's collection of representative image stacks of single cell types within the third instar larval *Drosophila* ventral nerve cord (VNC), and V3D software for reconstruction and registration to theoretical landmarks, we have made significant progress in generating the first digitally reconstructed fly segment.

Table of Contents

Introduction

Neuromics

A century ago, Ramón y Cajal mapped out the morphology of many isolated neurons, but with recent technology, we are beginning to map out neuromes. Neuromes represent the morphology of every neuron in a brain or ganglion, providing information on all neuronal types in that brain. In placing a neurome's entire set of reconstructions into a shared digital space by warping them to common landmarks, we will soon have morphological reconstructions of entire ganglions and brains. The creation of global neuronal maps of model organisms is an important first step in understanding the brain, especially if we believe Cajal's hypothesis that "all computation is anatomical" (Koch and Segev, 2000).

Cajal's hypothesis was furthered in 1943 when McCollough and Pitts demonstrated that with a large number of simple neurons wired together, universal computation can be performed. Each synapse can be thought of as a positive number, or synaptic weight. The activity of each presynaptic neuron is then multiplied by its synaptic weight, and these are summed. If the sum exceeds threshold, then the neuron fires and is said to be on. If not, then it is off. Consequently, networks of units with linear thresholds such as these, like binary code, can perform any computation a computer can (Koch and Segev, 2000). If the function of neuronal networks is based primarily on form as hypothesized, morphological and connectivity maps could provide deep insight into neuronal computation processes.

Connectomics

Past the neurome, scientists seek to map out the connectome, the entire network of neuronal connections in an organism. As yet, this has only been achieved with the female *C. elegans*, by Sydney Brenner's Nobel Prize winning team, over the course of a decade (1980s). The map was a massive undertaking that solidified *C. elegans* as one of the best understood model organisms, acting as a foundational tool for further developmental and behavioral research (Condron, B.G. 2010) (White et al., 1986).

With light microscopy, we can tell which neurons are in contact with one another, but this does not mean they are connected through synapses. Instead, Brenner's team used electron microscopy in a technique now known as dense mapping to work out the 300-neuron *C. elegans* wiring diagram. In dense mapping, the tissue is manually cut into extremely thin serial sections (50 nm at the thinnest) and imaged to create 3D stacks. However, because of this 50nm limit in z-resolution, axons can be very difficult to trace when they run parallel to the z plane, as they are often less than 100nm in diameter (Seung, 2009). In spite of these issues, Brenner and his team painstakingly located every synapse within *C. elegans*, and traced both the presynaptic and postsynaptic neurons back to their respective cell bodies. Nevertheless, 10% of the connections presumed were incorrect, and will soon be corrected with higher resolution imagery.

This method of mapping has not been extended to more complex organisms, simply because the time commitment would be so extreme. However, recent advances in automation not only boost the speed of the process one hundred fold, they improve the z-resolution significantly. For instance, SBFSEM (serial block face scanning electron microscopy), developed by Winfried Denk and his team, uses a diamond knife microtome

to cut slices as thin as 25 nanometers in z-depth (a resolution that can support even the most thin neuronal processes). (Helmstaedter et al., 2008). Thus, connectomes for the male and larval *C. elegans* will likely be completed within a few years, rather than another decade (Seung, 2009).

Although dense mapping is currently too laborious for more complex systems, a method using light microscopy for connectomics, dubbed sparse mapping, has entered the field. In this method, transsynaptic tracers are used to spread from one neuron to another, labeling the pre and postsynaptic neurons. These tracers are often genetically modified viruses, such as rabies, that lack the glycoprotein caps to spread across more than one synaptic cleft, thereby labeling only directly connected presynaptic neurons. Rabies virus has also been used similarly in vitro, and in vivo experiments will likely take place within a few years.

While these techniques are indeed fast, they are not nearly as reliable as dense reconstruction. For instance, it is unknown whether these transsynaptic markers always cross synaptic barriers, or whether they are occasionally blocked off. It is also unknown whether markers like the virus can spread to neurons that are merely in proximity, rather than synaptically paired to one another. A larger issue is that multiple animals will always be required for sparse reconstruction, as only a subset of neurons can be visualized at once, and multiple instances of connectivity must be found per pair for verification. The problem grows worse when attempting to find the connectivity of rare cells, and very large sample sizes must therefore be used. Staining methods can also be inconsistent, perhaps missing cell types altogether.

Sebastian Seung defines sparse and dense mapping modalities in a helpful manner. In sparse mapping, we create a database of neuronal types, find a synapse, and then identify the partners participating in that synapse by their type. We then repeat this observation across many samples for certainty. However, in the process of dense mapping, neuronal types do not need to be known. Potentially, the entire connectome can first be reconstructed and deciphered by EM, and subsequently, neuronal types could be derived numerically from this data (Seung, 2009).

Sparse mapping will be a much faster approach to connectomics for many years, but dense mapping is more reliable, and has greater potential; EM technologies will likely outstrip sparse mapping methods in time (Seung, 2009). For many years, however, these two methods will work in tandem. Generation of a neurome may soon become a day's work, or less, for advanced automation. With registration to landmarks, neuromes could be used to expedite dense mapping, by highlighting areas of neuronal overlap where synapses are probable.

Databases of neuronal types could also serve as measures of branch variation, allowing researchers to create probability maps. These maps would quantify which regions of a given neuron are highly variable and which regions are fixed. The data could then be compared to EM reconstructions, and let researchers know the normality of the neurons in their dense map. Such a "truth base" could also be used to teach automation to quickly classify reconstructions by type, and to recognize mutants as such.

Caveats

There are still several major issues open to debate in neuromics and connectomics. For instance, a firm definition for "neural type" must be reached. Many

researchers hold to the classical definition: shape and position of the neuron. On the other hand, many researchers argue electrical and genetic data should be used to further classify types. Similarly, the definition of synapse is still under debate. Physical connections between neurons often exist that are completely inactive, known as silent synapses. These are nonfunctional until specific developmental times or unique conditions. These lines blur further when considering the many neurons that discharge neurotransmitter into intercellular spaces, activating neighbors within the vicinity. Arguably, all affected partners are participating in a synapse. Additionally, tight and gap junctions can only be imaged by EM in certain orientations, and so many connections go unnoticed. It is unclear what combination of physical, electrical, and chemical interactions should deemed a synapse, and how many times two neurons must be connected for that synapse strength to be considered significant. These issues need to be resolved as the field of connectomics matures; a field that, by definition, makes claims about neuronal types being connected to one another. "Type" and "connection" are vague terms that must be clarified before they can serve as foundations.

Drosophila as a Model Organism

A wealth of physiological, morphological, and genetic information is known about *Drosophila*. In addition, the neurons in this system are orders of magnitude greater in complexity and variability than *C. elegans*. In particular, the *Drosophila* larval system holds the greatest potential for a deep understanding, and even control of, behavior. Its global structure is simple, yet the neurons within are intricate and diverse. Additionally, high generation time allows for large sample sizes and faster imaging. The ventral nerve cord (VNC), analogous to the spinal cord, controls waves of segmental contraction for

the animal's movement, and receives a great deal of sensory input as well. The VNC is bilaterally symmetric, and near-identical segments are repeated throughout the cord. Thus, if we can understand one hemisegment, we also come close to understanding the cord as a whole. For these reasons, modeling *Drosophila* is an ideal choice for neuroanatomists.

Fasciclin Bundles as Landmarks in Modeling Studies

Another feature that makes the *Drosophila* larval system attractive is the good characterization of neuronal territories within the VNC. In 2003, Landgraf et al. marked a set of axonal bundles using anti-FasciclinII antibodies, and discovered that these bundles were conserved structurally and positionally across embryonic-larval development, and across specimens. The authors encouraged other researchers to use these bundles as territorial dividers and landmarks in their own modeling studies, so a common language for neuronal classification in relation to the bundles could be developed (see figure 6 for details). Each segment of the *Drosophila* VNC has a slightly different shape, but with the same neuronal types. Thus, in order to compare the positions of neurons from one animal to another, each piece would need to be structurally warped onto a set of stereotypical fiduciary points, and the FASII bundles are ideal for this job. A good analogy for this warping process is a GPS system. GPS technology references fiduciary points, or satellites, and converts them to a universal coordinate map. This is what the FASII bundles are used for, and the result is an idealized global coordinate map for the reconstructions to occupy.

Reconstruction Overview

The field of neuroanatomy has been dormant for many years, but recent advances in computing and imaging technology are revitalizing efforts. With confocal light microscopy, we can image gigabytes of data in a single pass, producing image stacks that can be visualized in real-time 3D with many different software packages. Within the past five years, greater efforts to digitize these image stacks have begun. Digitization of neurons, also known as reconstruction, is the process of creating a computer model from a stack, effectively reducing gigabytes of data into a single file of a few kilobytes. This can be done manually, or as with newer software, in a semi-automated fashion. The benefit of the digital format is that models can be easily manipulated and shared, and even placed into a common 3D space to simulate neuronal interactions and global structures.

Tools for Reconstruction and Publishing

Development of software capable of semi-automated reconstruction is quite recent. Though still in its alpha testing phase, V3D purports to offer a 17-fold improvement in reliability, and a 10-fold improvement in speed over its competitor, Neurolucida (Peng et al., 2010).

NeuroMorpho.org has recently become the authority on the standards for digital reconstructions, and provides the largest online database for reconstructions to be published. It allows data search and download, and contains research across 10 species from 35 different scientists (Ascoli et al., 2007). Tools like these are revolutionizing the field of neuroanatomy, and allow the conduct of studies that would not have been possible just a few years ago.

Materials and Methods

Atlas of the Drosophila Ventral Nerve Cord (VNC)

1871 confocal image stacks of single GFP-labeled neurons (Chen and Condron, 2009) within the third instar foraging larval *Drosophila* VNC were obtained by Dr. Barry Condron and several undergraduates working in his lab. Labeling was achieved using a transcriptionally silenced GFP, unmasked by heat-shock expressed *flp* endonuclease. For each of several drivers, heat-shock times that produced approximately 5 labeled cells per VNC were determined empirically. Serotonin and FasciclinII costainings were also produced alongside the GFP staining (Condron et al., 2008). Stacks were grouped by criteria such as termination zones and GAL4s used to drive the GFP, revealing 33 distinct sensory neuronal types, 30 motor neurons, and 89 interneurons, roughly a complete VNC hemisegment (figure 1). At least two representative stacks were then selected for each of the 152 neuronal types; one stack was selected based on clarity, and the other was taken from the center of the cord, approximately at segment A4. Alongside the green GFP channel, red serotonin and blue fasciclinII channels were collected. These stains were used as landmarks for axes, and for warping of reconstructed neurons into register with one another (figure 6).

V3D Software and Neuronal Reconstruction

Collaborating with Dr. Hanchuan Peng, a software engineer at Janelia Farm, we tested early builds of V3D with the atlas. V3D is an application for real-time visualization of tiff stacks in 3D and semi-automated reconstruction of neurons. Though still in development, it is currently the most advanced tool available for stack manipulation and reconstruction (Peng et al., 2010). Most of the work on this project was

done in V3D alpha testing version 2.416, Nov. 2009, a build I found to be particularly stable and quick.

Representative stacks were first batch processed in Adobe Photoshop CS4 with levels and curves adjustments to maximize contrast, allowing V3D to more easily distinguish bright neuronal areas from black background; the bright areas are essentially the boundaries for the path followed through a trace operation (reconstruction). Markers were then placed at the origins of the neurons (cell bodies -- or axons entering from the periphery, in the case of the sensory neurons where the cell bodies were not imaged because they were removed in the dissection process) and at branch points and terminal arbors (figure 2). Tracing operations were performed for each pair of markers; for instance 1 → 2, 2 → 3, 2 → 4, and so on. V3D interpolates between these points, following the path of the branch and filling in volume, xyz coordinates, and connectivity, all of which are represented in the .swc file (a simple text document). In a later build of V3D, the "trace to all markers" function was added, allowing a greatly accelerated tracing workflow. In this way, at least one of every representative sensory and motor neuron stack was reconstructed (figures 3 and 4). In addition, four interneurons have been traced thus far (figure 5).

All reconstructed neurons were exported in the .swc format, the current standard for reconstructions, and the one required by NeuroMorpho.org, the largest database of neuronal reconstructions to date (Ascoli et al., 2007).

V3D 'Warp Pointset' Plugin

Dr. Peng had already developed warping tools, but not for our specific purpose. We needed an application that would warp completed .swc trace files to

common landmarks, thereby reforming and repositioning the trace files into their approximate real locations within the VNC by use of a theoretical standard; this technique would essentially conform one 3D mesh to another. The theoretical standard chosen was the FASII staining; fasciclin II marks axonal bundles that are positioned with little variation from cord to cord (Landgraf et al., 2003). Dr. Condron measured the positions of these bundles within 30 different larvae, generating a set of theoretical averages by which the dataset could be warped (figure 6).

Prior to warping, markers were placed at a maximum of 30 different positions within representative stacks; these were the ventrolateral, dorsolateral, central (tri-bundle), dorsomedial, and ventromedial bundles (thus, 5 per hemisegment). As the cord is bilaterally symmetric, there were a total of 10 bundles per segment to mark, and for each representative stack, we marked three segments, for a total of 30 possible markers. Marker positioning was confined to the horizontal planes where serotonergic axons cross the midline of the VNC and synapse on the contralateral side (a structure used to delimit one segment from the next) (figure 6). Although 30 markers per stack was our ideal, stacks were taken in different orientations, with differing ranges of z space, and various intensities of channels; it was rare for all bundles to be present within a given stack. Thus, in creation of the V3D warp pointset plugin, features were added to allow matching of any subset of markers to the theoretical standard. In this way, warping could be performed with fewer than 30 markers, though the greater number of markers the user provided, the more accurate the operation would be. Using this novel warping plugin, 14 sensory neurons were put into register with one another, accurately reflecting their approximate VNC locations (figure 8).

Figure 1

10,000 image stacks of isolated sensory, motor, and interneurons were collected from the third instar foraging *Drosophila* larval ventral nerve cord (VNC). 5,000 of these stacks were used to create a database of neuronal types, and at least two representative stacks were selected for each type. Approximately 33 sensory neuron, 30 motor neuron, and 89 interneuron types were found, though this data is still subject to change. Here we see top-down views of representative stacks from all 33 sensory neurons – original data by Dr. Condron. Compare to figure 3.

Figure 2

A: Approximately 1200 markers were placed throughout this motor neuron. Markers represent points in three-dimensional space that are used by V3D to perform trace operations. This is done by path-finding and edge detection along the neurites, and constant volume estimation. Essentially, V3D interpolates points and volume between markers. **B:** Here, reconstruction was performed one trace operation at a time, taking three weeks to complete. This was before inception of the "trace to all markers" function, which greatly expedited the process. **C:** The reconstruction (.swc file) is isolated from the stack. **D:** A 180° flip of the neuron about the X-axis is shown for a more complete depiction of the structure. **E:** Midline information, or the central trace lines in the branches, can be viewed in V3D or in cvapp (as pictured), an application for processing and upload to NeuroMorpho.org. Midline information does not include volume.

Figure 1 - Atlas of *Drosophila* VNC (Sensory Neurons)

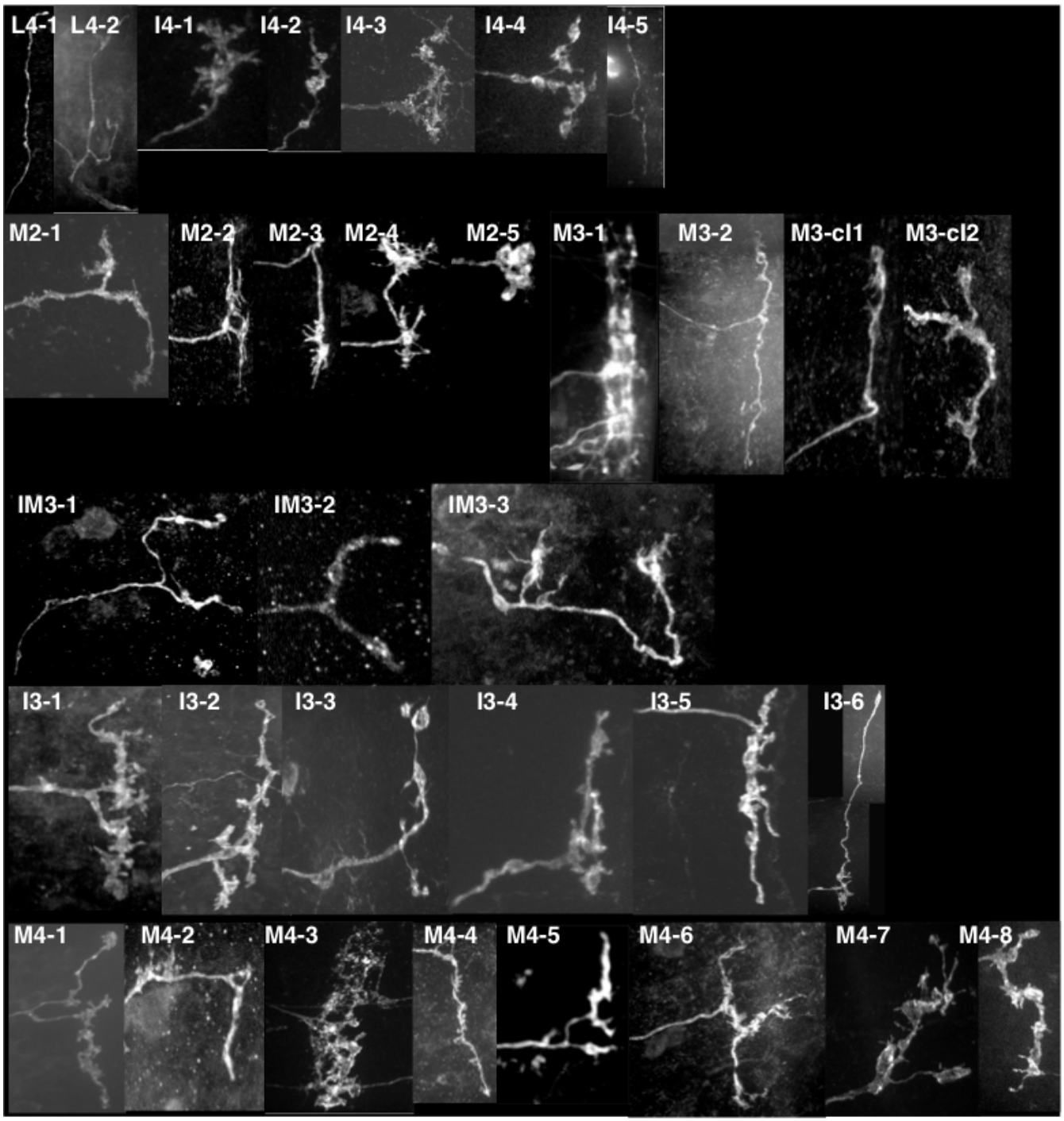

Figure 2 - Tracing (Digital Reconstruction)

A. **Markers Placed**

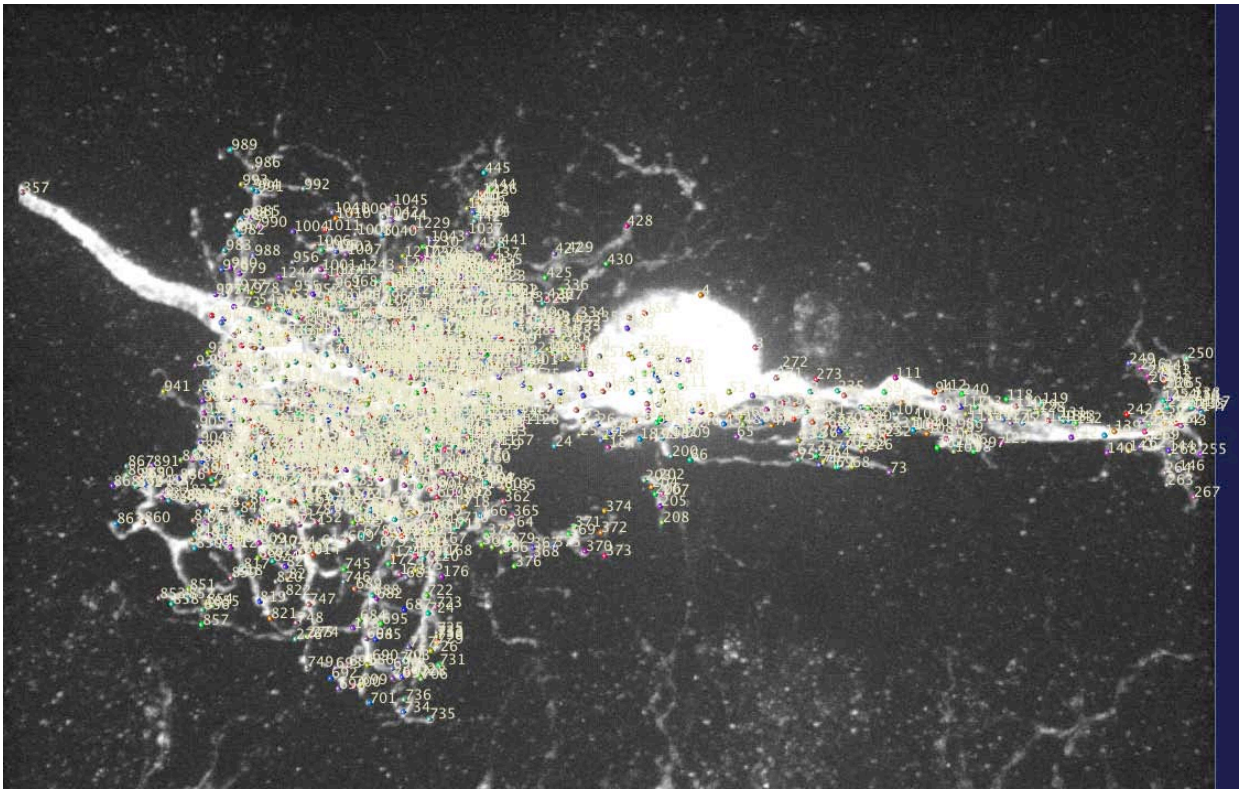

B. **Reconstruction and Stack**

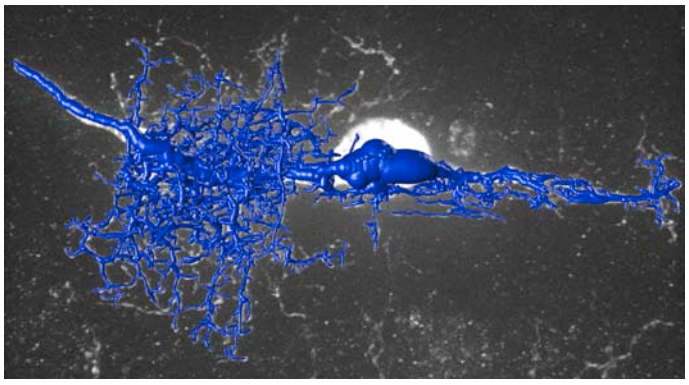

C. **Reconstruction Isolated**

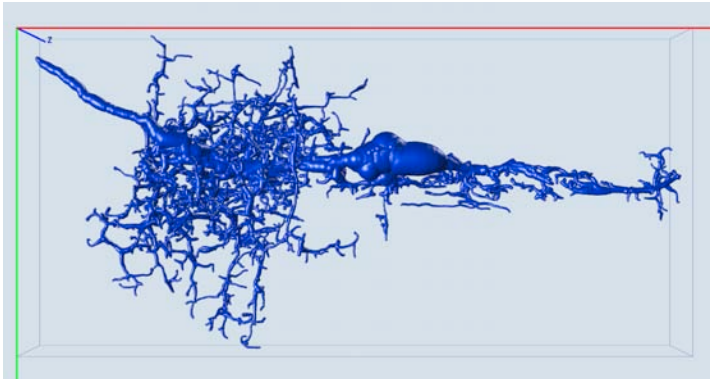

D. **180° Rotation About X**

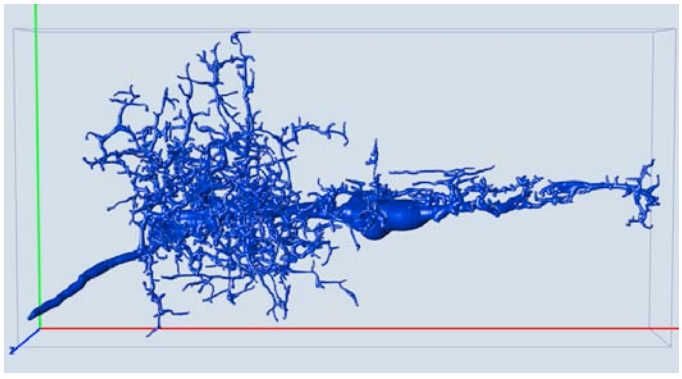

E. **Reconstruction Midlines**

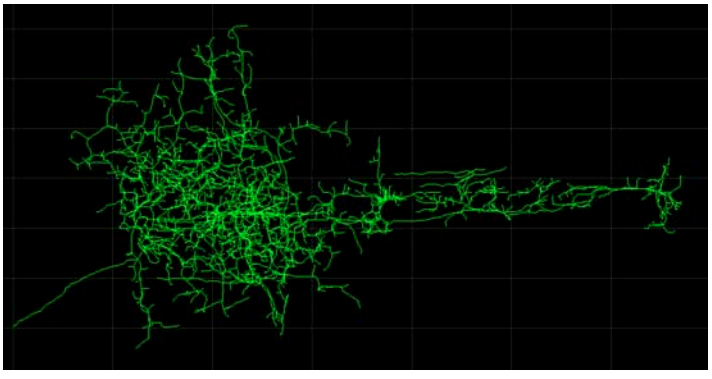

Results

Software Troubleshooting and Development

Much of the initial work on this project was simple exploration of V3D and discussion with Dr. Peng until we could reliably import stacks and trace neurons. The steps toward this function were not obvious, and builds of V3D we received often did not include tracing functionality, or suffered from other errors. However, this was to be expected, as V3D is still in its alpha testing phase.

We placed several feature requests with Dr. Peng that improved our use of V3D, including one that would let us swap the root-tip order of segments within the .swc trace files, formatting them appropriately for NeuroMorpho.org, so that they can later be added to the online database (Ascoli et al., 2007). Initially, there was no viable method of saving the .swc files in an editable format, so motor neuron traces (or any complex trace) were quite difficult; they had to be generated all at once. If the application crashed, all work on that neuron would be lost. Thankfully, this was solved within a couple months of the start of our project.

V3D has added some very fast and efficient tools to the community, and is expansible by addition of plugins, encouraged by Dr. Peng. A touted feature of the program is its ability to trace neurons in real-time 3D, that is, setting markers and tracing using only the 3D viewer, and rarely falling back on the 2D slice display. Consider for a moment what this entails – users must be able to place markers into the 3D stack on the fly, and if there are other neuronal densities behind the intended target, V3D must somehow parse these and select the correct location for the marker. This is done by several means, some of which are still in development. One simply allows the user to

draw in branches with a mouse or stylus, and V3D will correct user strokes as they go, matching them to the intense target areas. Another method lets users right click to lay down a marker, and V3D takes its best guess by placing it at the depth below the click where intensity is greatest. If this proves inaccurate, users can specify that V3D interpret after two or three clicks. This means that the target is selected, followed by rotation of the stack, then selection of the target again, so that V3D can interpret the desired location by use of both angles. Selections can also be winnowed by only allowing V3D to see certain portions of the stack – temporary cropping, if you will.

These tools are quite useful, and prove to be efficient on small trace operations like the sensory neurons. However, by examining figure 2, it is obvious that such tools become burdensome when dealt such extreme complexity. Manipulating image stacks in 3D also requires a great amount of processor power, and with large datasets like ours, this workflow is not feasible on most computers. Thus, V3D is currently best suited to users with small datasets and high-end computers. Due to this focus, the 2D tools have gone by the wayside, and need significant improvement before this program can be the ubiquitous visualization and reconstruction tool the developers intended.

In our dialogue with Dr. Peng's team, we played the role of alpha-testers by helping to refine V3D, and will continue to do so as long as we work on reconstruction projects. We also participated in the development of novel software that registers reconstructions to a theoretical dataset within a shared 3D coordinate space.

Trace Fidelity

Once we had optimized a Photoshop → V3D workflow, we began systematically tracing the sensory neurons, as they are much simpler than the motor neurons. Much of

Figure 3

Reconstructions of all sensory neuronal types within the VNC are displayed here. Note that only the axons, dendrites, and terminal arbors are present, as cell bodies in the periphery are removed during the dissection process. Through this figure, one can gain an appreciation of the high level of variation present in the nerve cord.

Figure 4

Reconstructions of all motor neuronal types are shown. Note the increased complexity of these neurons as compared to the sensory types. Cell bodies are all present, and structurally, neurons in the VNC are monopolar.

Figure 5

Here we see reconstructions of four interneurons. The serotonergic neurons **(A and B)** are used as structural landmarks for orientation and warping. The cell bodies are in the ventral region of the cord. View figure 6 for a stain of these neurons. **A:** Medial serotonergic neuron. **B:** Lateral serotonergic neuron. **C:** An additional two characteristic interneuronal types.

Figure 3 - Sensory Neurons

L4-1

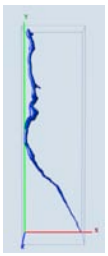

L4-2

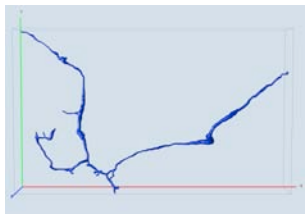

I4-1

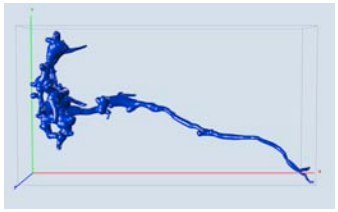

I4-2

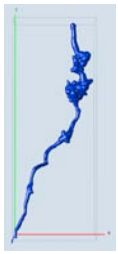

I4-3

I4-4

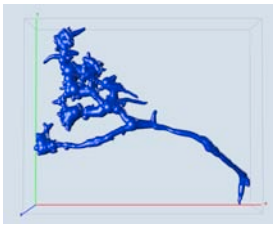

I4-5

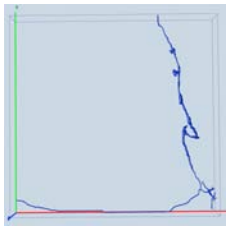

M2-1

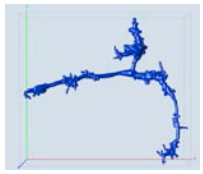

M2-2

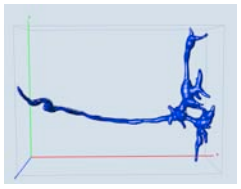

M2-3

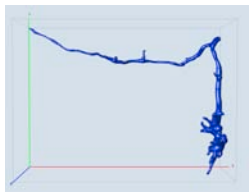

M2-4

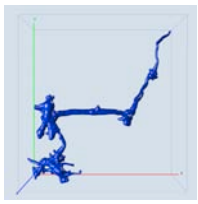

M2-5

M3-1

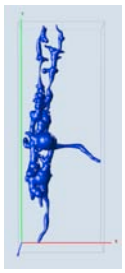

M3-2

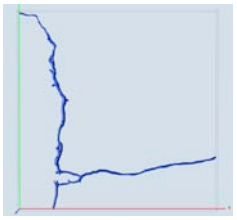

M3-cl-1

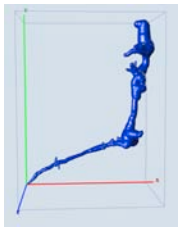

M3-cl-2

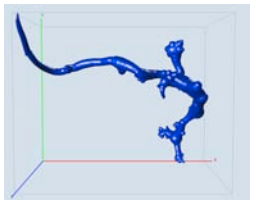

IM3-1

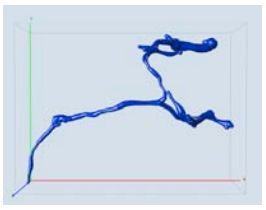

IM3-2

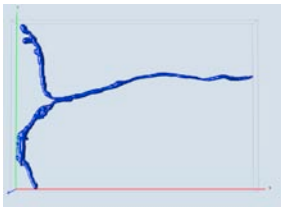

IM3-3

I3-1

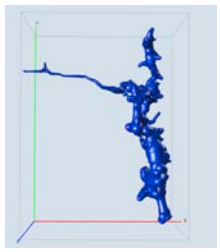

I3-2

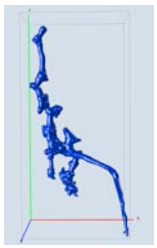

I3-3

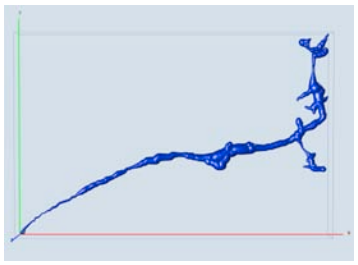

I3-4

I3-5

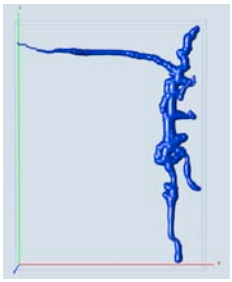

I3-6

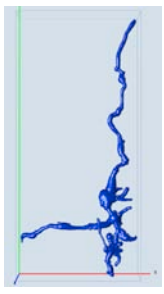

M4-1

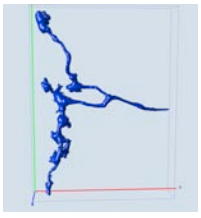

M4-2

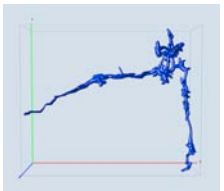

M4-3

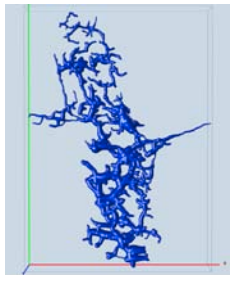

M4-4

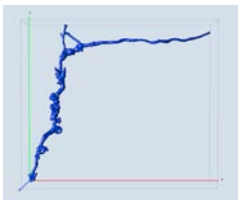

M4-5

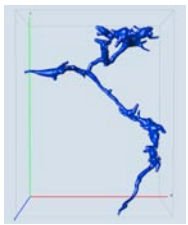

M4-6

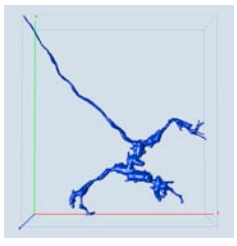

M4-7

M4-8

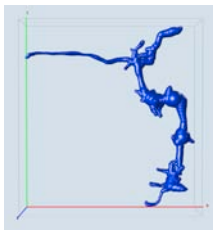

M4-9

Figure 4 - Motor Neurons

mn-1

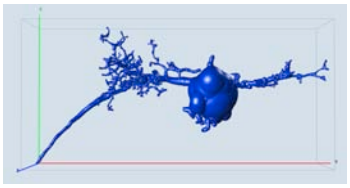

mn-2

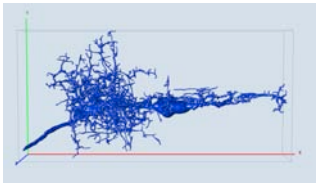

mn-3

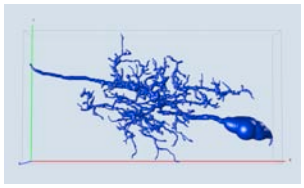

mn-4

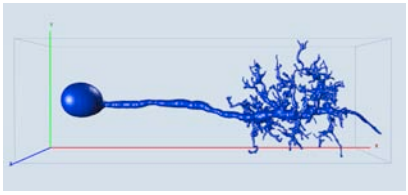

mn-5

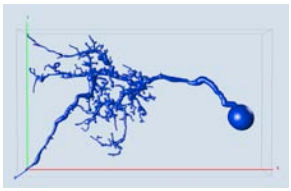

mn-6

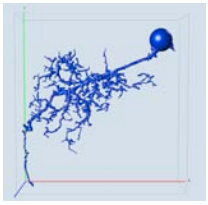

mn-7

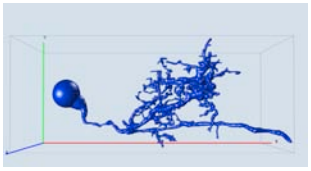

mn-8

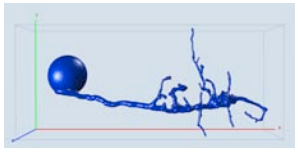

mn-9

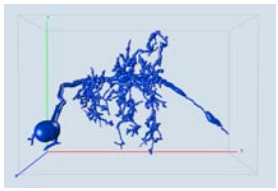

mn-10

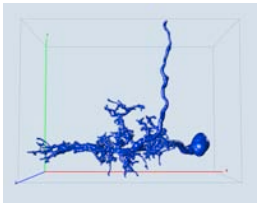

mn-11

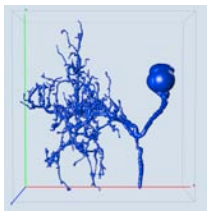

mn-12

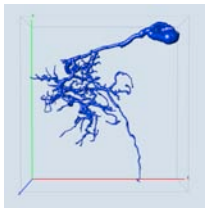

mn-13

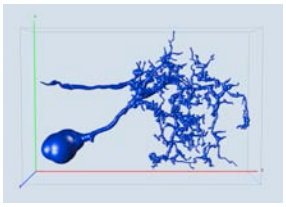

mn-14

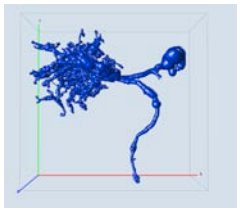

mn-15

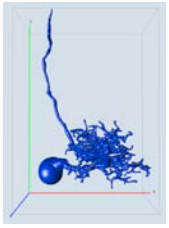

mn-16

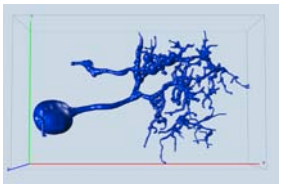

mn-17

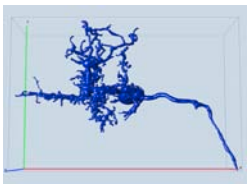

mn-18

mn-19

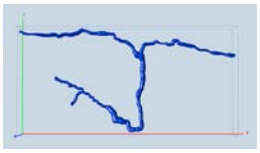

mn-20

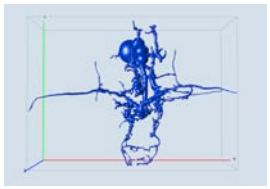

mn-21

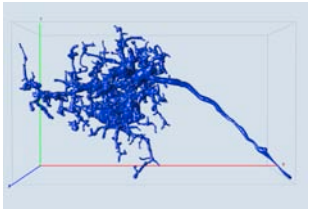

mn-22

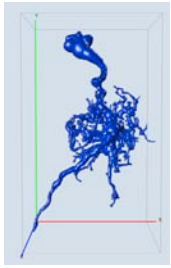

mn-23

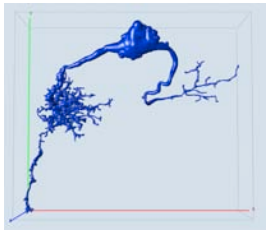

mn-24

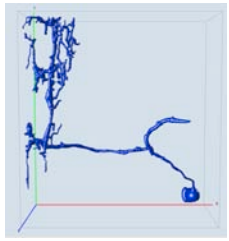

mn-25

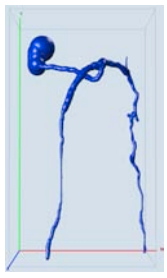

mn-26

mn-27

mn-46

mn-122

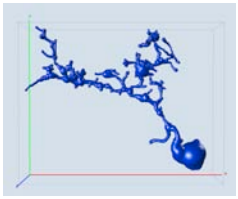

mn-124

Figure 5 - Interneurons

A.

Characteristic Medial 5HT Neuron

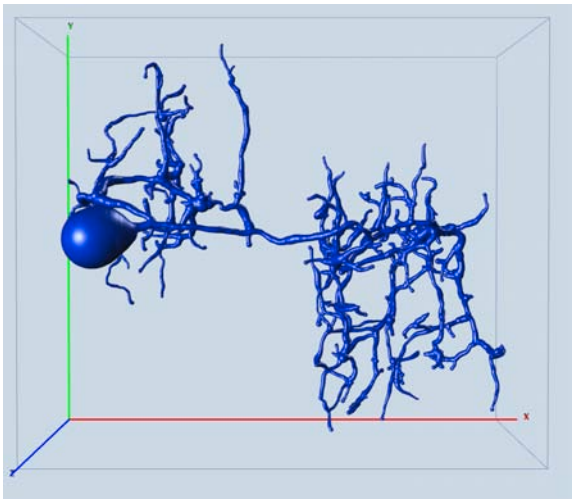

Front View (Rotate 90° About X Axis)

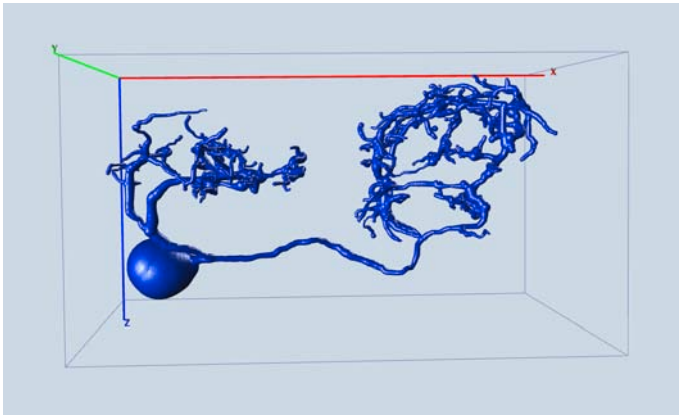

B.

Characteristic Lateral 5HT Neuron

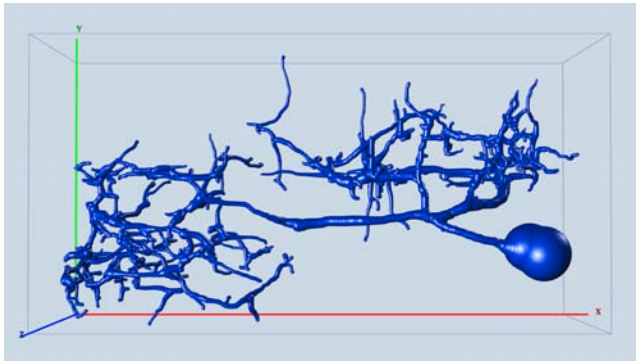

Front View (Rotate 90° About X Axis)

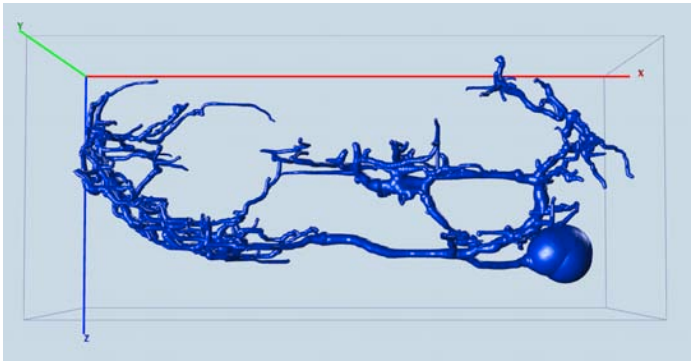

C.

in44

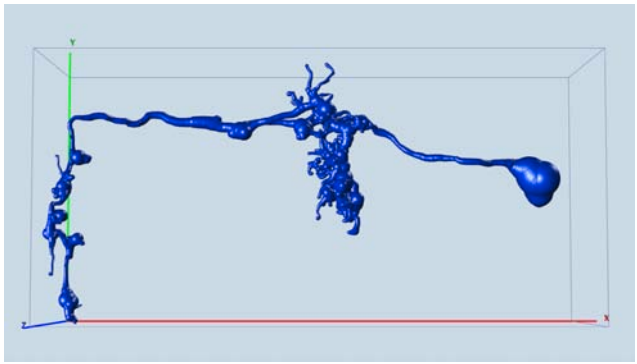

in40

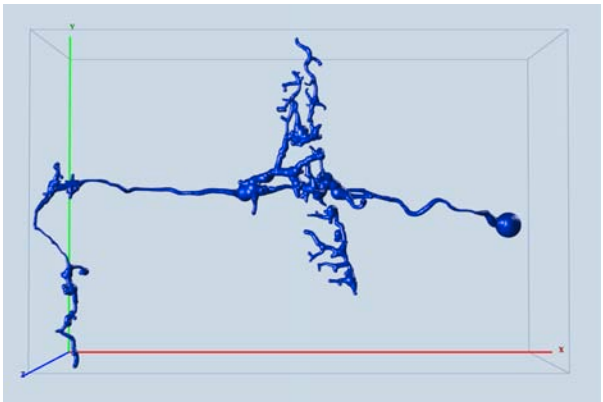

V3D's performance, as it turns out, is dependent upon the contrast and noise within the stacks, so adjustments in Photoshop play a large role. If the contrast is low, then V3D will interpret gray pixels as additional volume, and the reconstructions will suffer from lack of detail and expanded boundaries. On the other hand, if care isn't taken with the curves adjustment, portions of the image can easily be lost. This occurs when medium luminosity pixels (more faint branches) are interpreted as below threshold, and thus reduced to black. If the contrast curve is too steep, or is in the wrong portion of the histogram, serious data loss can occur. So, before tracing each neuron, we compared high contrast adjusted copies of the stacks to low contrast, to make sure little or no data loss was occurring. Thus, high contrast stacks could be given to V3D for optimal tracing without concern.

Most stacks traced quite accurately, as seen in figure 9. In figure 2, the cell body, dendrites, and axon of a very complex motor neuron are all clearly visible. In fact, this reconstruction represents approximately 1200 markers and separate trace operations. The issues that did occur with tracing often had to do with stacks of very few z slices; V3D has trouble filling in areas that are wide horizontally but with little depth. Additionally, certain stacks contained neurons that where the 'flip out' GFP procedure did not sufficiently isolate them from surrounding neurons, and in these cases it was extremely difficult to tell which branches belonged to which neurons (Chen and Condron, 2009) (Sykes and Condron, 2005). Occasionally, large parts of the neuron such as the cell body or dendrites were partially or completely cropped out. These problems can be seen in figure 9. The solution at this point is simple – more data collection.

Digital Registration

The first test of the warp pointset plugin was to take multiple instances of the same neuronal type and warp all of them to the theoretical landmarks, as seen in figure 7. The unwarped compilation shows how scattered the traces are, especially in z space. They are also randomly oriented, as some stacks are taken from top to bottom and others from bottom to top (resulting in flipped dorsoventral axes); the anteroposterior axes are also inconsistent. Thus, when the .swc files are successfully warped and put back into the same digital space, they align with consistent A/P and D/V axes, and correct xyz positions within the virtual cord (figure 7). In addition, they group into three segments, as shown. Occasionally, the cord is skewed diagonally, or deformed in specific positions. Warping takes care of these cases as well and distorts the .swc file to match the difference between registered fiduciary points in the stacks and the theoretical standard. This distortion follows Hooke's Law of elasticity, that the displacement of a spring is in direct proportion with the load added to it. Each voxel, or three-dimensional pixel is treated as a point with six springs attached to neighboring voxels, such that one spring exists per vector (X, -X, Y, -Y, Z, -Z). Thus, the fiduciary points from the FASII bundles of a representative stack are pulled in three-dimensional space to match the theoretical FASII bundles, and the 3D mesh containing the reconstruction is distorted to match the theoretical landscape along with the bundles.

Roughly 1/3 of the stacks have inadequate serotonergic stains in which the axons crossing the midline, cell bodies, or both, are not present. This prevents us from easily determining the orientation of A/P and D/V axes in the stacks, and from positioning markers along the serotonergic midlines. There are likely workarounds to these issues,

Figure 6

A: Pictured here are the theoretical landmarks generated by Dr. Condron after measuring the position of FASII bundles in 30 different animals and averaging. On the left, three segments are displayed: S-1, S, and S+1. On the right we see the abbreviated names for the FASII bundles: D stands for dorsal, V for ventral, C for central, R for right, L for left, and I for intermediate. These points represent an idealized cord, and the digital landscape that the reconstructions are warped into. **B:** the FASII bundles are shown in an actual cord. Note how this cord is slightly skewed. The .swc structure will be corrected against this skew after warping. In this cord, all ten FASII bundles are present, a rarity in itself. Even so, notable variation is present in the width of the cord and path of the bundles. For this reason, theoretical bundles, as in **A**, are preferable. **C:** Markers are positioned according to the FASII bundles. **D:** The serotonergic (5HT) channel is added to show how markers are placed along the horizontal planes where the 5HT neurons cross the midline and synapse on the contralateral side.

Figure 7

Here we see five separate neurons of the same type (I4-3), before and after warping. Before warping, these neurons are in random dorsoventral and anteroposterior orientations, and arbitrary positions within the cord, as images stacks are all taken at different orientations and offsets. Thus, the pre-warp collection of neurons does not closely resemble reality. Post-warp, however, neurons are brought into the approximate regions in which they exist in nature. **A:** Top-down view. **B:** Side view (90° rotation about the X-axis) **C:** The neurons come together into three separate virtual segments after warping. Now, the difference between blue and orange, and between yellow and green, more closely represents natural variation.

Figure 6 -Warping Preparation

Top-Down View

Front View (90° Rotation About X Axis)

A.

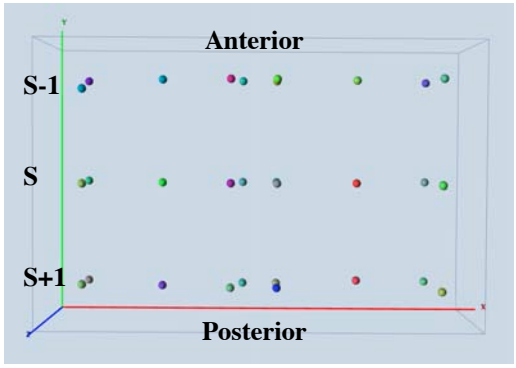

Theoretical Landmarks

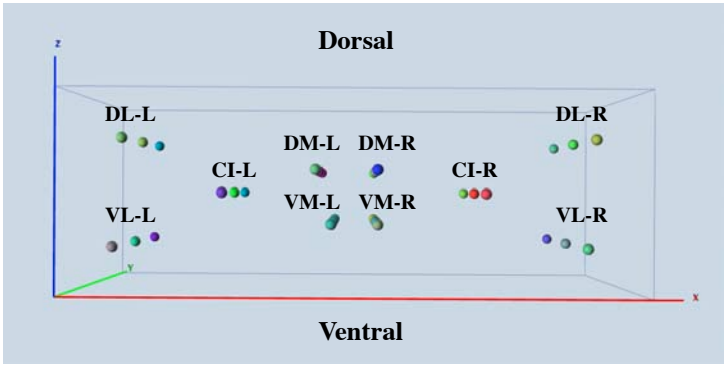

B.

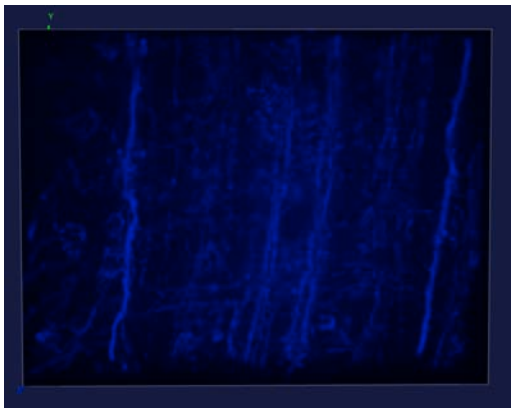

FASII Staining

C.

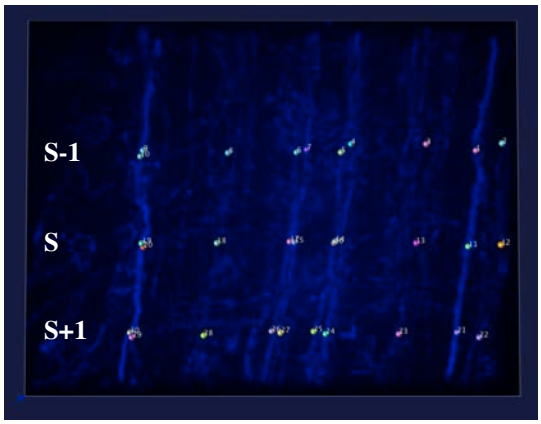

Fiduciary Markers Added

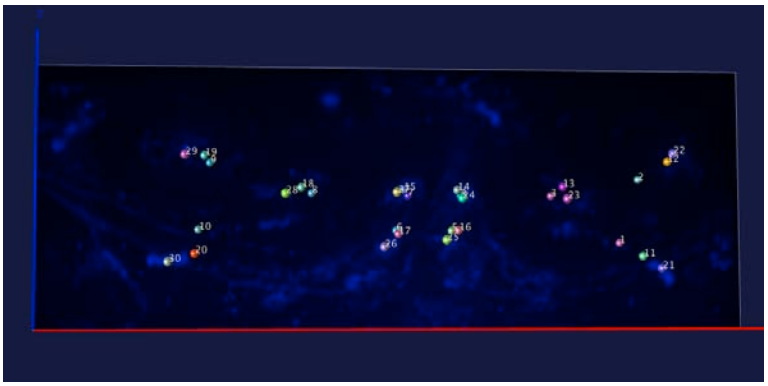

D.

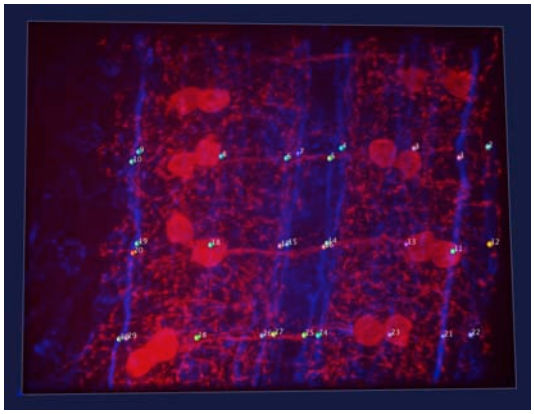

5HT (Serotonin) Staining Overlaid

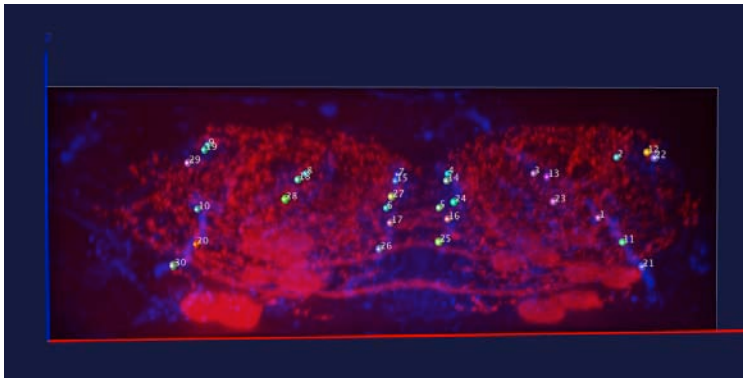

Figure 7 - Five I4-3 Neurons Warped

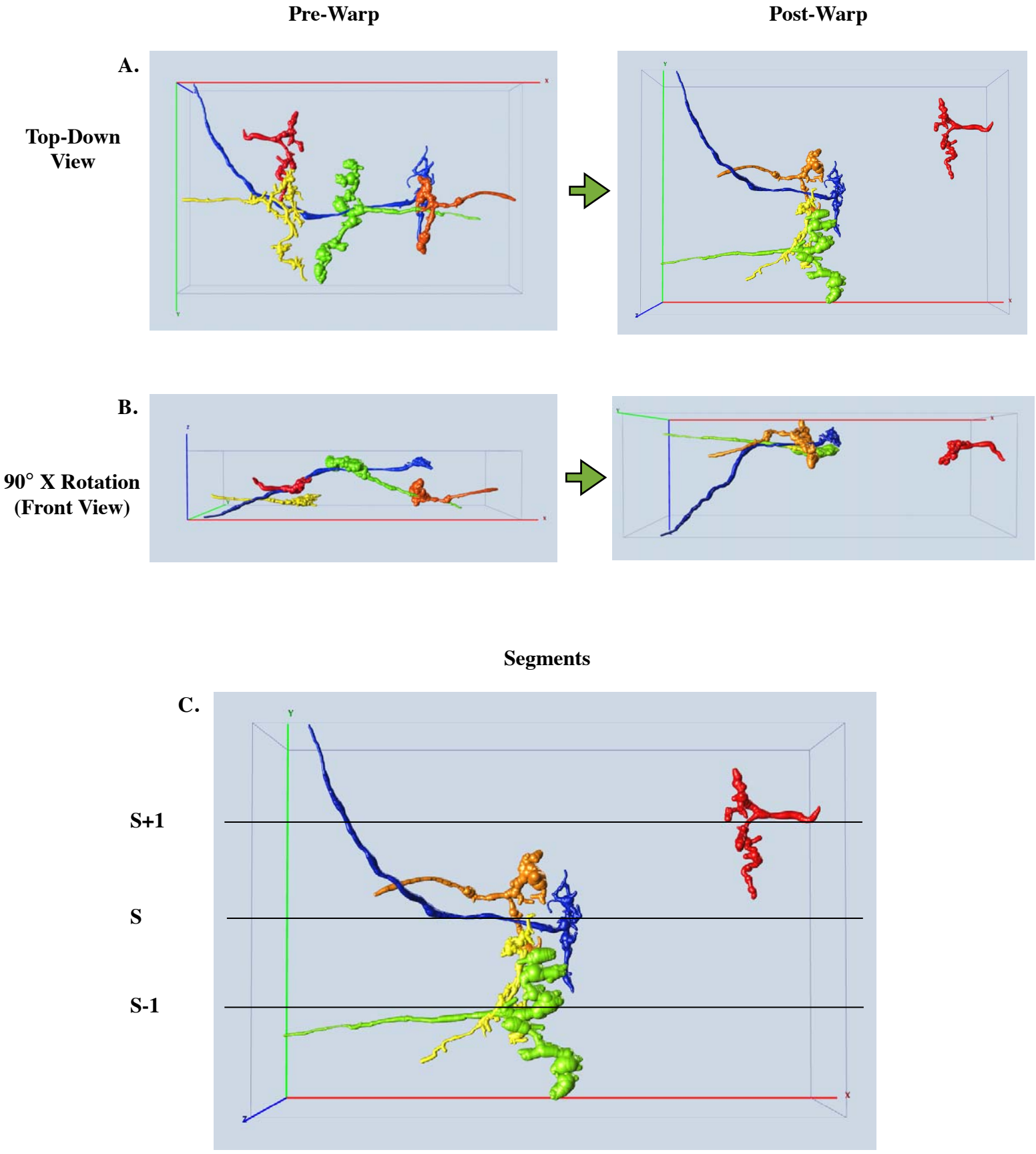

Figure 8

A: 14 sensory neurons are added to the same digital space. After warping, they approximately match their literal positions within the VNC. The warping algorithm takes the fiduciary points from the FASII bundles of a representative stack and aligns them with the theoretical bundles, pulling the 3D mesh space of the reconstructions in line as well. In this way, the post-warp reconstructions are all in registration with the theoretical bundles. **B:** FASII bundles from one representative cord were traced as a reference point for this example. They were then warped to the shared theoretical dataset so they could be included in the warped neuron 3D space. Note, however, that these bundles are not idealized, but are simply used to illustrate general position in the cord. **C:** A 90° rotation about the X-axis, this view best demonstrates how well the neurons are ordered post-warp.

Figure 9

Here we see examples of accurate and poor tracing. **A:** An interneuron with superb trace fidelity. **B:** A motor neuron with highly complex branching, especially in z-depth. Note, however, that V3D has issues when tracing wide and shallow densities. The cell body in this figure appears full from the top-down view, but when rotated to the side in **C**, it becomes apparent that most of it was cropped off. This is why V3D's interpretation of the cell body does not seem to closely match the image from the top, but is in fact accurate upon further inspection. **D:** Again, V3D has trouble filling densities when they are wide and shallow, as is the case with the motor neuron in this figure. Neighboring neuronal density is also too high to decipher precisely which branches belong to the target neuron, and the cell body is cropped off, causing additional problems. For these, we will rate the tracing quality as poor and search for additional representative stacks.

Figure 8 - Warping (Registration)

Pre-Warp **Post-Warp**

A.

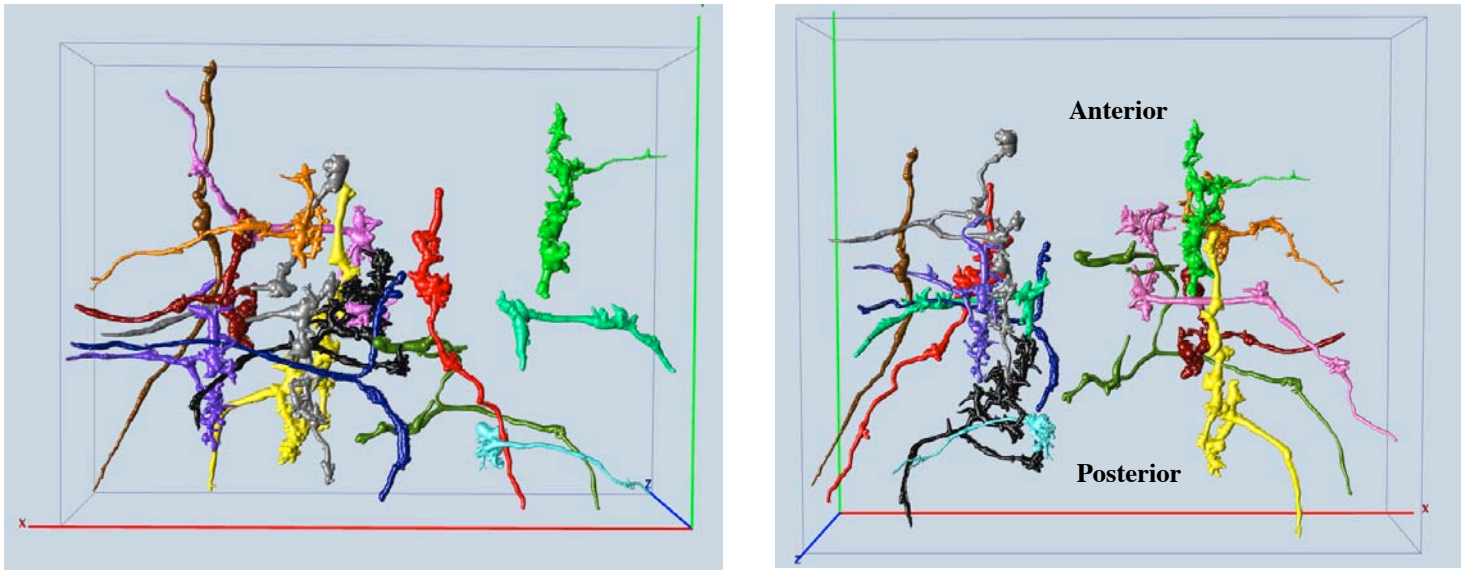

Traced FasII Bundles Added **FasII Bundles Warped**

B.

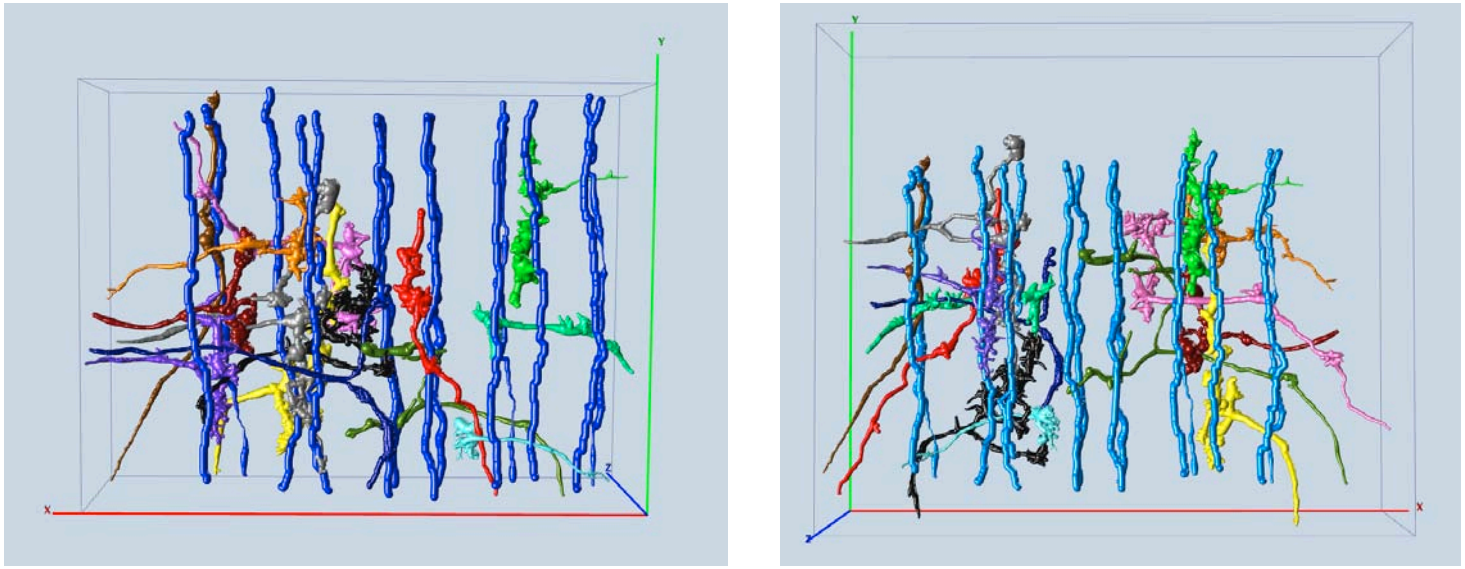

90° X Rotation

C.

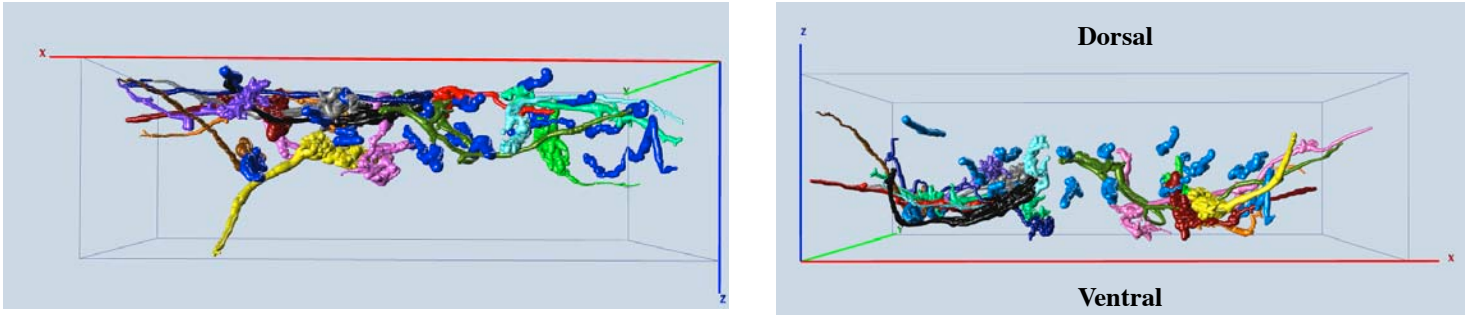

Figure 9 - Trace Fidelity

Good Fidelity

Pre-Trace **Post-Trace**

A.

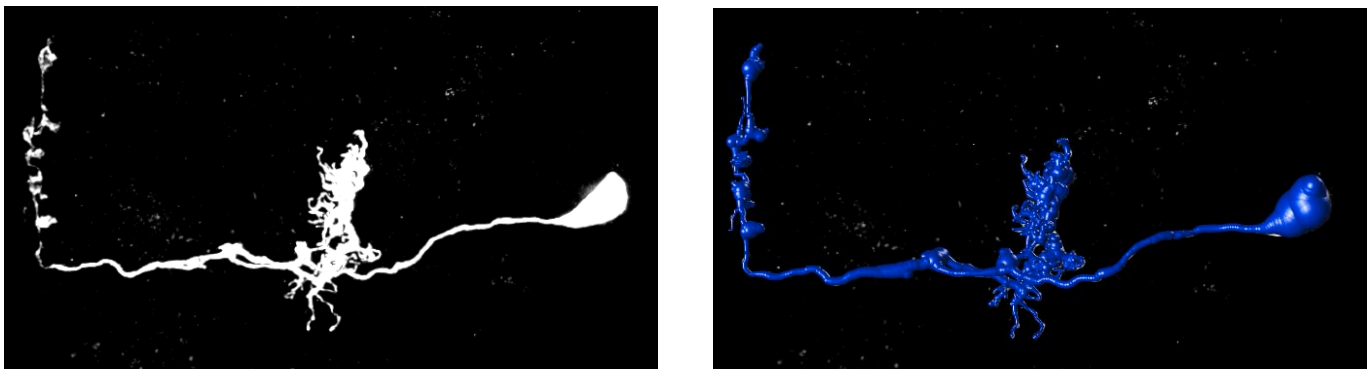

B.

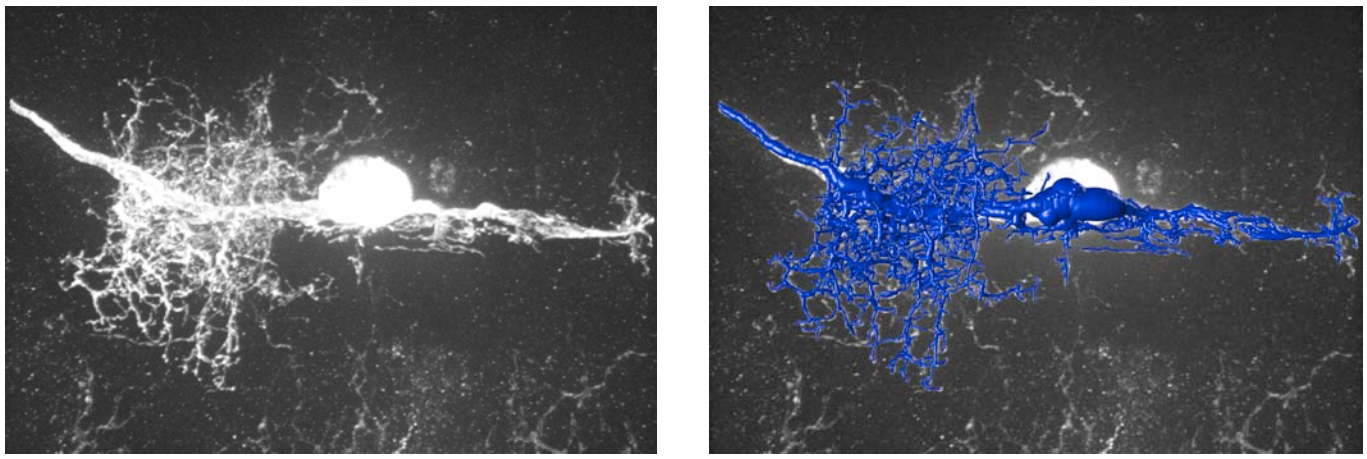

C.

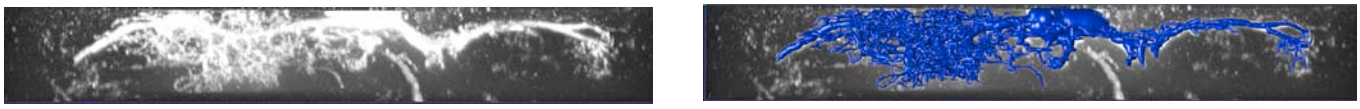

Poor Fidelity

D.

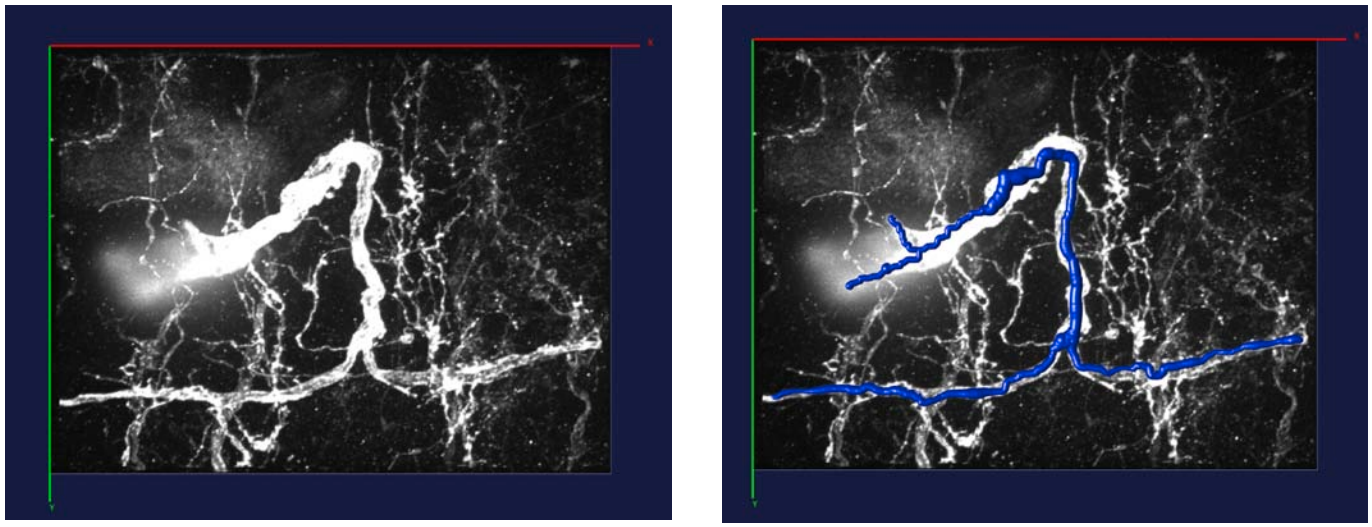

but the data presented here is recent, so only the most clear-cut stacks have been used. None of the motor neurons have yet been warped, as the issues mentioned above are more common among these stacks. When the motor neurons are compiled without warping, the dendrites are so thick that not much global structure can be observed, but perhaps warping will create some order from the chaos.

The greatest issue with our model thus far is variability. Artificial variance is introduced at every step of the process: dissection may skew cords, damage neurons, and release factors that change neuronal architecture. Fixing (mounting with paraformaldehyde) the tissue similarly introduces a great deal of variation, and staining intensity is also inconsistent. Contrast adjustment in Photoshop, imperfect trace fidelity, and imperfect warping also introduce variability. For all these reasons, it becomes difficult to determine whether variations are natural or induced, and so we must develop a more standardized approach to the entire workflow. Eventually, researchers may be able to image these tissues *in vivo*, which would solve many of these problems.

Conclusions

Although we have not yet delved into study of the *Drosophila* connectome, when completed, this project will represent the first complete digital ganglion of a complex organism. Our focus is on morphological characteristics and variation, and accurate placement of reconstructions into a common 3D coordinate space. Interestingly, this digital ganglion also represents, with a few exceptions, the entire ventral nerve cord. The 152 known neurons per hemisegment are mirrored on the contralateral side, and segments

Figure 10

Here we see a depiction of the neuronal variation present within a single cell type, in this case mn-2. In **A**, dendritic arborization is minimal, but as the images progress to **D**, arborization increases dramatically. As the collection of stacks for each neuronal type is expanded, variation will become measurable, and work on variability maps will begin. A variability map will demonstrate which branches of the neuron are fixed in their positions, which branches vary in a predictable manner, and which vary so greatly as to appear random. From this data, computers may soon be trained to auto-trace and instantly categorize these traces into their respective neuronal types. Such data may also be highly valuable to scientists working on EM reconstruction, and provide insight into the classification and normality of any neuron in question, as variability data would take far too long to collect through EM.

Figure 10 - Neuronal Variation (mn-2)

Top-Down View **Front View**

A.

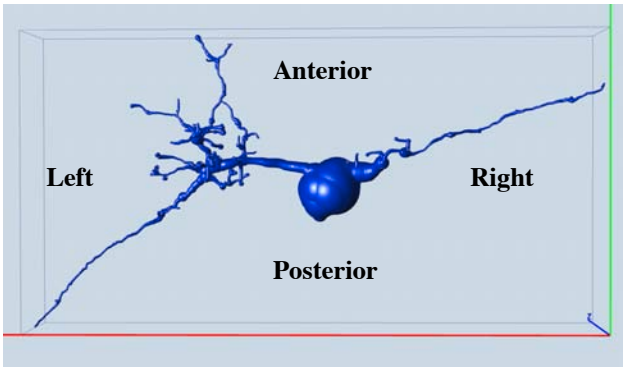

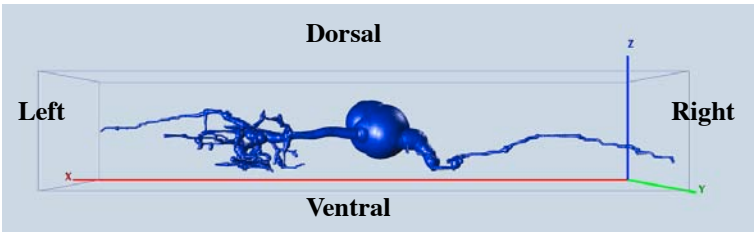

B.

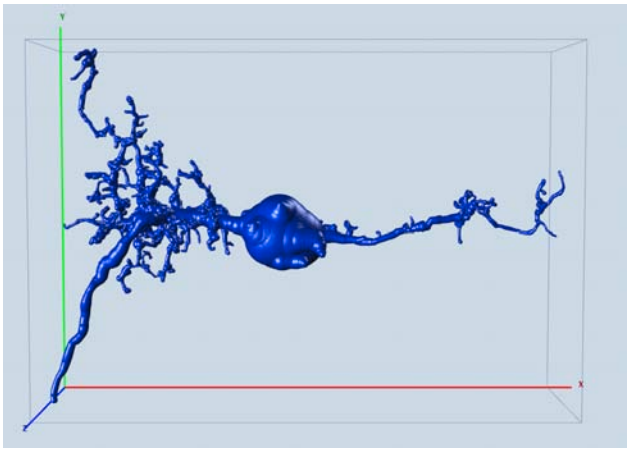

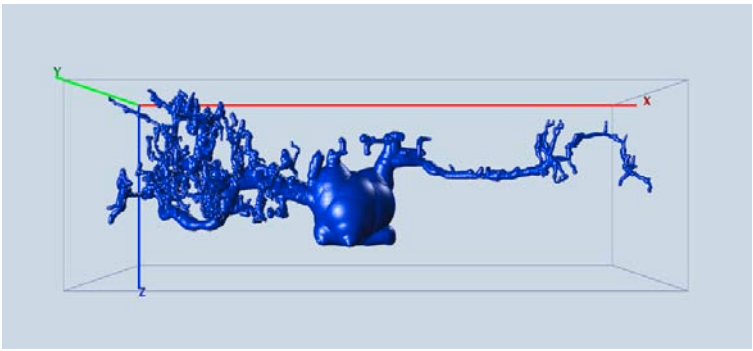

C.

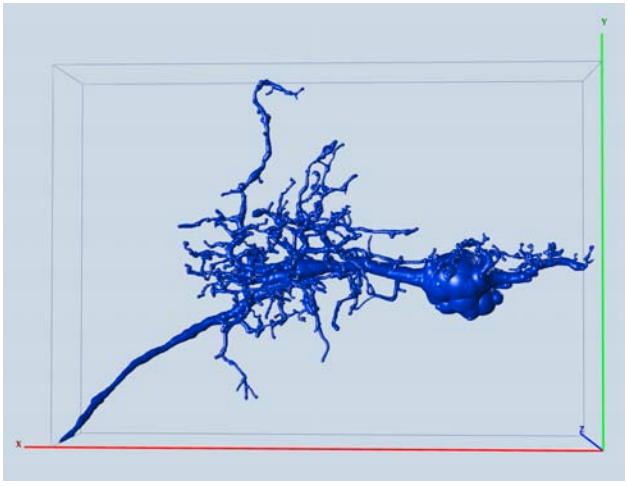

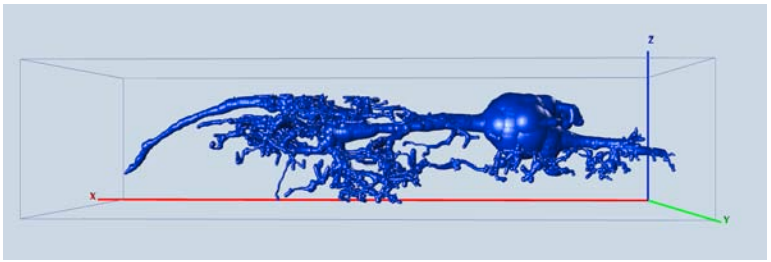

D.

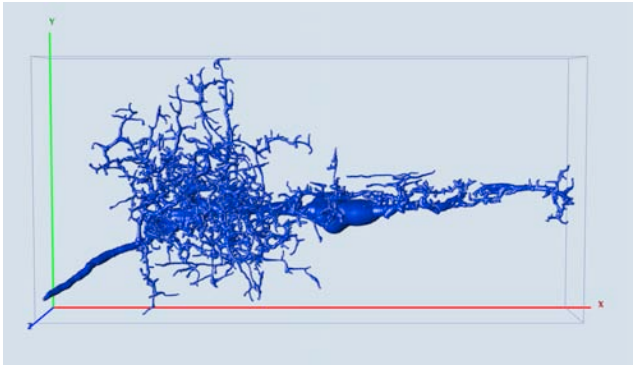

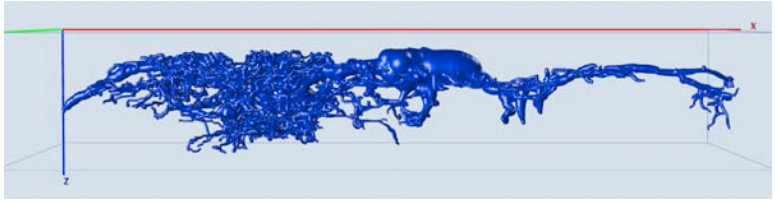

are presumed to be near identical to one another. Thus, in our structural analysis of one hemisegment within the VNC, we reach near-complete analysis of the entire cord.

This dataset could prove useful for several reasons. First, although many reconstructions are made publicly available through NeuroMorpho.org, none are ensemble sets of any part of the CNS like ours. Thus, our project could provide a good template for future modeling studies of this kind.

Structural models can also be utilized to answer various biological questions. For instance, one group of researchers used a reconstructed *Drosophila* neuron, combined with computer-generated dendrites of varied complexity, in electrical modeling. They simulated signal propagation using this electrical model, running trials from the soma and dendrites, approximating the necessary spacing and positions of synaptic events for large EPSPs to occur (Gouwens and Wilson, 2009). Hence, experiments in virtual systems, or *in silico* studies, can be used as a testing ground to expedite the process of making real-world findings.

Although our project may generate some interest from researchers who also work on the *Drosophila* larval CNS, or ganglia in similar organisms that coordinate movement by segmental waves, the primary users will probably be educators. An appreciation of neuronal diversity can be gained by viewing of this project, and once the reconstructions are all warped into a common 3D space, global cord structure will also be apparent. Color schemes can be applied to demonstrate both general diversity, and differences between sensory and motor regions. Videos of the digital ganglion could easily become useful and popular tools for educators (Condron, 2010).

Although several caveats remain, exploration of these problems could prove to be fascinating. For instance, the neurons from the atlas are taken from a great number of specimens. Are all 152 neurons per hemisegment present in each organism, or are there some neurons that are optional? As seen in figure 10, diversity between neurons of the same type can be great, so would a second digital ganglion look very much like the first? Additionally, all images used in this project were from the third instar larval foraging stage (L3F). Perhaps there are neurons specific to certain stages of development; this could mean that the types defined in the atlas apply only to L3F. We know that during the pupal stage of development, serotonergic neuron branches decline severely and regrow later in pupation (Chen and Condron, 2008). Occurrences of neuronal death and regrowth are common in *Drosophila* development, so it's unclear how much variation would be present between ganglions at differing phases, and whether the neuronal types defined here could translate to other phases. These questions all warrant investigation through additional digital models, alongside further development of reconstruction and warping technology.

As we set our sights on organisms of greater complexity, such as the mouse, and eventually, the human, automation speed and competence will become the limiting factor. For instance, if we were to attempt to decipher the connectome of the human brain at this stage by manual reconstruction using SSTEM, it would take 3 billion work years per cortical column (Helmstaedter et al., 2008). This is not surprising, as the human brain contains 100 billion neurons and 100 trillion synapses. Dense mapping techniques must increase in speed one million fold before the human connectome can be deciphered.

Mapping the brain will likely become a massive effort, on the scale of the human genome project, but before we can even proceed to the *Drosophila* cortex, technology must improve. Automation will be key, and several groups of software engineers are already engaged in work on this problem. Most promising thus far is the development of artificial intelligence that can follow humans as they trace neurons, learning as they go to mimic their behavior, but not to "take their mistakes too literally" (Eisenstein, 2009). Another key factor will be tools like Brainbow, where different mixtures of fluorescent proteins (GFP, RFP, YFP, CFP) coalesce in neurons to create up to one hundred distinguishable colors (Helmstaedter et al., 2008). This technology allows staining (and therefore reconstruction) of at least 75% of the organism at once. Brainbow is therefore essential when working with animals like the mouse that require small sample sizes. More importantly, using Brainbow, we can identify the origin and termination zones of neurons simply by their unique color, without having to follow the length of their processes in between. This may prove extremely useful to researchers working on the connectome.

Connectomics discoveries will likely produce many new fields of research. For instance, "connectopathies," or problems in axon guidance, could turn out to be responsible for many disorders we see today. Even with more simple neurome data, studies on neurodegenerative disorders could be conducted. By reconstructing a series of brains (even in simple organisms such as *Drosophila*) at different developmental periods (or, for instance, with overexpressed Alzheimer's-producing genes), we may discover that certain groups of neurons are prone to degrade before others. Unlocking the intricate structure and connectivity map of the brain will be a giant step forward for science, and if

memories are stored as a mesh of connections, as is now believed, then we may also be able to finally decode the language of memory, cognition, and consciousness.

References

Ascoli, G. A., Donohue, D. E. & Halavi, M. NeuroMorpho.Org: a central resource for neuronal morphologies. J Neurosci 27, 9247-51 (2007).

Chen, J. & Condron, B. G. Branch architecture of the fly larval abdominal serotonergic neurons. Developmental Biology In Press, Accepted Manuscript (2008).

Condron, B. G. CRCNS data sharing: A digital atlas of the neurons of the Drosophila larval ventral nerve cord. Pending NSF Grant (2010).

Condron, B.G, Wolfe, A., & Yang, Y. An atlas of *Drosophila* larval abdominal neurons used to identify targets of excess serotonin. (2008).

Eisenstein, M. Neural circuits: Putting neurons on the map. Nature 461, 1149-52 (2009).

Gouwens, N.W., Wilson, R.I. Signal propagation in Drosophila central neurons. J Neurosci 29, 6239-49 (2009).

Koch, C. & Segev, I. The role of single neurons in information processing. Nat Neurosci 3 Suppl, 1171-7 (2000).

Helmstaedter, M., Briggman, K.L., & Denk, W. 3D structural imaging of the brain with photons and electrons. Curr Opin Neurobiol 18, 633-641 (2008).

Landgraf, M., Sanchez-Soriano, N., Technau, G. M., Urban, J. & Prokop, A. Charting the Drosophila neuropile: a strategy for the standardised characterisation of genetically amenable neurites. Dev Biol 260, 207-25 (2003).

Peng, H., Ruan, Z., Long, F., Simpson, J.H., & Myers, E.W. V3D enables real-time 3D visualization and quantitative analysis of large-scale biological image data sets. Nat Biotechnol 28, 348-53 (2010).

Seung, S. H. Reading the Book of Memory: Sparse Sampling versus Dense Mapping of Connectomes. J. Neuron 62, 17-29 (2009).

Sykes, P. A. & Condron, B. G. Development and sensitivity to serotonin of Drosophila serotonergic varicosities in the central nervous system. Dev Biol 286, 207-16 (2005).

White, J. G., Southgate, E., Thomson, J. N. & Brenner, S. The Structure of the Nervous System of the Nematode Caenorhabditis elegans. Philosophical Transactions of the Royal Society of London. Series B, Biological Sciences 314, 1-340 (1986).

Acknowledgements

I'd like to thank Barry Condron for being an excellent mentor for over a year, and for smartly placing me on a project that fit my interests for both computers and neurobiology. I'd also like to thank Christopher Deppmann, and Sarah Kucenas for their comments on my paper and their general enthusiasm and openness to discussion about the work.